Available online at www.sciencedirect.com
SCIENCE DIRECT
Biochemical and Biophysical Research Communications 340 (2006) 633–638
BBRC
www.elsevier.com/locate/ybbrc

Lipid membrane interaction and antimicrobial activity of GsMTx-4, an inhibitor of mechanosensitive channel

Hoi Jong Jung [a], Pyoung Il Kim [b], Seung Kyu Lee [a], Chul Won Lee [a], Young-Jae Eu [a], Dong Gun Lee [c], Yung-E Earm [d], Jae Il Kim [a,*]

[a] Department of Life Science, Gwangju Institute of Science and Technology, Gwangju, 500-712, Republic of Korea
[b] Division of Microbiology, National Center for Toxicological Research, Food and Drug Administration, Jefferson, AR, USA
[c] School of Life Science and Biotechnology, College of Natural Sciences, Kyungpook National University, 1370 Sankyuk-dong, Puk-ku, Taegu 702-701, Republic of Korea
[d] Department of Physiology, Seoul National University, College of Medicine, 28 Yonkeun-Dong, Chongno-Ku, Seoul 110-799, Republic of Korea

Received 26 November 2005
Available online 19 December 2005

Abstract

GsMTx-4, a polypeptide from the spider *Grammostola spatulata*, is an inhibitor of mechanosensitive channels. It is known to interact with lipid membranes, suggesting it partitions into the membrane to alter the channel gating, but the effect of the membrane charge on GsMTx-4 activity remains unknown. In this study, we found that GsMTx-4 more effectively interacts with anionic lipids than zwitterionic ones. The effect of GsMTx-4 on negatively charged membranes was similar to that of the antimicrobial peptide melittin, which led us to assess GsMTx-4's antimicrobial activity. Interestingly, we found that, in contrast to other neurotoxins, GsMTx-4 exhibited antimicrobial properties and was more active against Gram-positive than Gram-negative bacteria. These results suggest that GsMTx-4 exerts its antimicrobial effect by altering the packing of the membrane and/or inhibiting mechanosensitive channels. These findings could point the way towards a new class of antimicrobial peptides.

Keywords: GsMTx-4; Mechanosensitive channel; Channel inhibitor; Antimicrobial peptide

Mechanosensitive channels (MS channels) serve as sensory transducers, converting a mechanical stimulus at the membrane to an electrochemical response. Recently, it was reported that GsMTx-4, a peptide isolated from the venom of the Chilean rose tarantula *Grammostola spatulata*, specifically inhibits MS channels in astrocytes and kidney cells [1,2]. This 34-amino acid peptide contains three intramolecular disulfide bonds that form a cysteine knot motif, which is a highly efficient motif for structure stabilization. Toxins containing this motif exhibit a broad range of biological activities. For example, Tachystatin A found in the Japanese horseshoe crab inhibits the growth of Gram-negative and Gram-positive bacteria and fungi [3,4].

Toxins targeting ion channels have been divided into two major classes based on the domain of the channel with which they interact and their mechanism of action. The first class is made up of pore blockers, which interact with the external vestibule of the conduction pore, thereby blocking the flow of ions [5–14]. The second class contains gating modifiers, which interact with the voltage-sensing domains of voltage-gated channels. Examples of gating modifiers include SGTx, HaTx, VSTx1, and GrTx, which alter the gating behavior of Ca^{2+} and K^+ channels [15–19], as well as GsMTx-4. Such gating modifiers, including GsMTx-4, are usually amphipathic and partition into the membrane to alter the gating of ion channels [20,21]. Likewise, many antimicrobial peptides commonly exhibit

* Corresponding author. Fax: +82 62 970 2484.
E-mail address: jikim@gist.ac.kr (J.I. Kim).

0006-291X/$ - see front matter © 2005 Elsevier Inc. All rights reserved.
doi:10.1016/j.bbrc.2005.12.046

amphipathicity, which likely facilitates interaction with the bacterial membrane. We were therefore interested in the way in which membrane charge affects GsMTx-4 binding and whether or not it possessed antimicrobial properties.

Materials and methods

Peptide synthesis. The linear precursors of toxins were synthesized by solid-phase methodology of fluorenylmethoxycarbonyl (Fmoc) chemistry using a variety of blocking groups for the protection of amino acids. The synthetic peptides were deprotected and cleaved using a mixture (82.5% trifluoroacetic acid (TFA), 2.5% 1,2-ethanedithiol, 5% H_2O, 5% thioanisole, and 5% phenol, v/v) and then precipitated with diethyl ether. The deprotected linear peptides were diluted to a final peptide concentration of 2.5×10^{-5} M and subjected to oxidative disulfide bond formation at 4 °C for 3 days in 0.1 M ammonium acetate buffer (pH 7.8) containing 0.1 M NaCl and reduced/oxidized glutathione (molar ratio of peptide:GSH:GSSG was 1:100:10). The cyclization reaction was monitored by reverse-phase high performance liquid chromatography (RP-HPLC), and when complete, the reaction mixture was loaded onto CM-cellulose CM-52 column and eluted with ammonium acetate (pH 6.5). The purity of synthetic peptide was confirmed by analytical RP-HPLC and MALDI-TOF mass spectrometry.

Vesicle leakage experiments. Large unilamellar vesicles (LUVs) composed of POPG (1-palmitoyl-2-oleoyl-3-phosphoglycerol), POPC (1-palmitoyl-2-oleoyl-3-phosphocholine), and POPC:POPG (1:1, w/w) were prepared using the ether evaporation method in the presence of 70 mM calcein. Aqueous solutions contained 10 mM Tris buffer (pH 7.4), 150 mM NaCl, and 0.1 mM EDTA. The initially formed vesicles were extruded through a 0.4 μm Nuclepore filter. Untrapped dye was removed from the LUVs by gel filtration on a Sephadex G-50 column (1.5 ± 30 cm), using an eluant of 10 mM sodium phosphate buffer (pH 7.4) containing 150 mM NaCl. The separated LUV fraction, after appropriate dilution to a final concentration of 3.34 μM, was mixed with the peptide solution for 3 min in a 2 ml quartz cuvette at 25 °C. The leakage of calcein from the LUV was monitored by measuring the intensity at 520 nm after excitement at 490 nm on a Shimadzu RF-5000 spectrofluorometer (Tokyo, Japan). The percentage of dye release caused by each peptide was calculated by the following equation: % leakage $= 100 \times (F - F_0)/(F_t - F_0)$, where F_0 is the initial fluorescence intensity, F_t is the total fluorescence intensity observed after the addition of 20 μl of 10% Triton X-100, and F is the fluorescence intensity in the presence of the peptide.

Reverse-phase high performance liquid chromatography. Purified toxins were monitored by RP-HPLC with a linear gradient at a flow rate of 1 ml min^{-1} from 20% to 60% mobile-phase B over 40 min, where mobile-phase A was 0.1% TFA in water and mobile-phase B was 100% acetonitrile and 0.1% TFA. Eluted toxins were analyzed by MALDI-TOF mass spectrometry.

Antimicrobial activity. Escherichia coli (KCTC 1682), *Salmonella typhimurium* (KCTC 1926), *Pseudomonas aeruginosa* (KCTC 1637), *Bacillus subtilis* (KCTC 3068), *Staphylococcus epidermidis* (KCTC 1917), and *Staphylococcus aureus* (KCTC 1621) were supplied from the Korean Collection for Type Cultures (KCTC). Briefly, single colonies of bacteria were inoculated into the culture medium (LB broth) and cultured overnight at 37 °C. An aliquot of this culture was transferred to 10 ml of fresh culture medium and incubated for an additional 3–5 h at 37 °C to obtain mid-logarithmic-phase organisms. A 2-fold dilution series of peptides in 1% peptone was prepared, and serial dilutions (100 μl) were added to 100 μl of $2–4 \times 10^6$ CFU/ml in 96-well microtiter plates (Falcon) and then incubated at 37 °C for 16 h. The inhibition of growth was determined by measuring the absorbance at 620 nm with a Microplate ELISA Reader (Molecular Devices, Sunnyvale, California). The lowest concentration of peptide that completely inhibited growth of the organisms was defined as the minimal inhibitory concentration (MIC). The MICs were the average of measurements in three or six independent assays.

Results and discussion

Interaction between GsMTx-4 and phospholipid membranes

Previous studies have shown the importance of the mechanical properties of the lipid bilayer for proper MS channel function [22,23]. The first significant evidence of an effect of the lipid membrane profile on channel activity was the finding that the activity could be modulated by certain amphipathic compounds and anesthetics [24]. Consistent with that idea, alteration of the pressure profile using phospholipids with shorter acyl chains dramatically altered the mechanosensitivity of MscL channels (MS channel of large conductance) [25]. In that regard, when applied to the extracellular face of the cell membrane, GsMTx-4 inhibits channel activity by increasing the membrane tension required for activation [1]. In the present study, to know the effect of the membrane charge on GsMTx-4, we examined the ability to elicit release of the fluorescent dye calcein from LUVs comprised of zwitterionic (POPC), partially anionic (POPC:POPG), and purely anionic (POPG) phospholipids by altering the lipid packing. The self-quenching properties of this dye cause its fluorescence intensity to be much weaker when entrapped within vesicles than when free in aqueous solution. Consequently, perturbation of the phospholipid lipid packing that results in escape of the dye is detectable as an increase in fluorescence that is proportional to the amount of dye released. Leakage of 100% of the dye was defined by the addition of Triton X-100, which completely disrupted the vesicles.

We found that GsMTx-4 released calcein from all three vesicle types and interacted efficiently with negatively charged POPG LUVs rather than zwitterionic POPC LUVs by as much as about 400-fold (100% calcein leakage from POPG at 0.04 μM; 100% from POPC:POPG (1:1) at 0.16 μM; 80% from POPC at 16 μM) (Figs. 1A–C). In the solution structure determined by NMR, GsMTx-4 is composed of a large hydrophobic patch and a number of charged residues (Fig. 2). All of the charged residues (Lys8, Lys15, Arg18, Lys20, Lys22, Lys25, and Lys28) are favorably oriented for solvent accessibility, and the regions of positive electrostatic potential are situated on the opposite side of the molecule from the assembly comprising the hydrophobic surface (Phe5, Trp6, Trp7, Leu26, Phe27, Leu29, and Phe32). With purely zwitterionic phospholipid vesicles, the predominant force of attraction between GsMTx-4 and membrane would be the hydrophobic interaction between the nonpolar face of GsMTx-4 and the lipid, whereas with anionic vesicles, it would be the favorable electrostatic interaction between the negatively charged lipid headgroup and the positively charged residues of the peptide. This combination of hydrophobic and hydrophilic residues of GsMTx-4 would provide that the toxin interacted efficiently with negatively charged POPG LUVs by the way in which the positively charged surface interacts with the negatively charged membrane

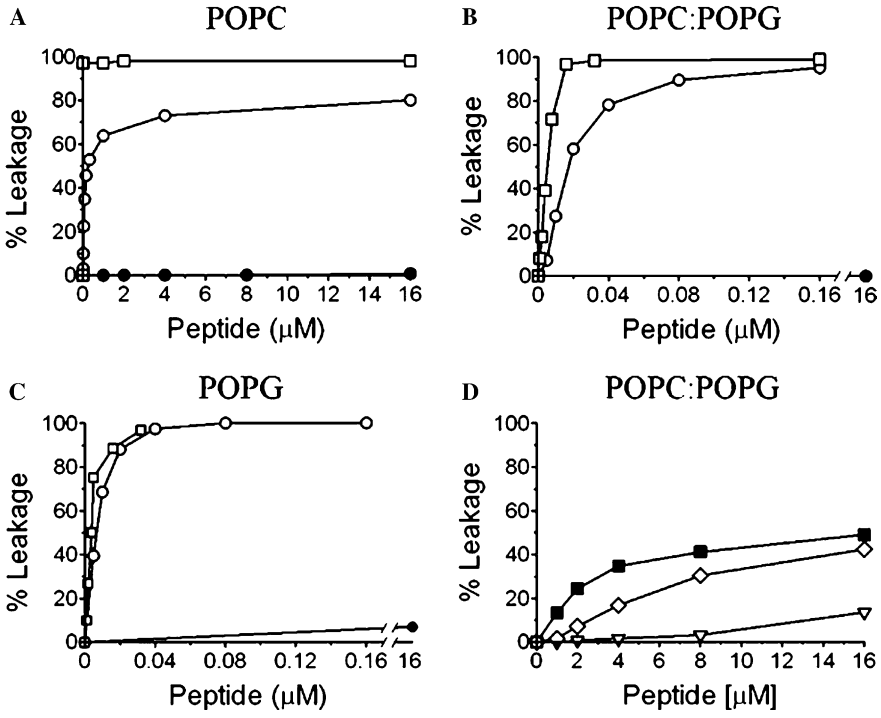

Fig. 1. Membrane interaction of toxins. Dose-dependent release of calcein from LUVs comprised of POPC (A), POPC:POPG (1:1) (B,D) or POPG (C) elicited by melittin (□), GsMTx-4 (○), GVIA (●), Vstx1 (∇), SGTx (◊), and GrTx (■).

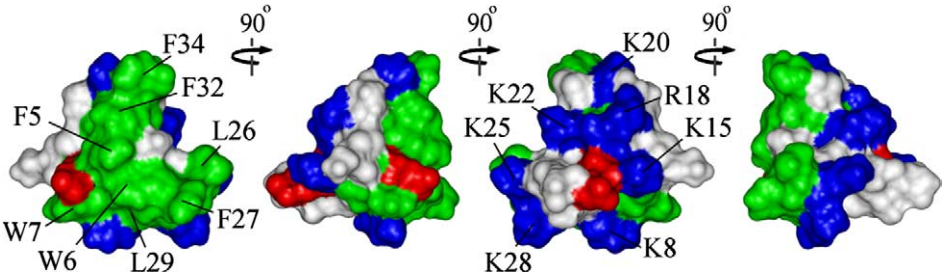

Fig. 2. Surface profiles of GsMTx-4 showing the hydrophobic patch and surrounding charged residues. Hydrophobic, basic, and acidic residues are colored green, blue, and red, respectively. GsMTx-4 has been deposited in the Protein Data bank (PDB entry 1LU8). (For interpretation of the references to color in this figure legend, the reader is referred to the web version of this paper.)

head groups, while the hydrophobic surface interacts with the nonpolar region of the membrane.

Many pore blockers interact with the external vestibule of the conduction pore to block the flow of ions as protein–protein interaction [5–14]. Although the backbone structures of the toxins are similar to that of GsMTx-4, the toxins have different surface features such as no hydrophobic patch and important charged residues for binding to the pore domain [5–14]. Consistent with the structural feature of the toxins, in calcein leakage experiment, a N-type Ca^{2+} channel pore blocker ω-conotoxin GVIA had no significant effect on the membrane under any conditions (Figs. 1A–C).

Melittin, a membrane targeting antimicrobial peptide, elicited calcein release from all of the POPC, POPC:POPG, and POPG LUVs (Figs. 1A–C). It indicates that melittin interacts with the membrane more independently of lipid charge. However, GsMTx-4 showed the different interaction between POPC and POPG LUVs. The lipid charge dependence on the ability of GsMTx-4 would be caused by the nonpolar interaction of the large hydrophobic patch. At RP-HPLC in which immobilized hydrocarbon chains served as the stationary phase, comparison of the surface hydrophobic regions of both GsMTx-4 and melittin revealed that the hydrophobicity of exposed nonpolar residues of melittin is much stronger than that of GsMTx-4 (Fig. 3). GsMTx-4 and melittin interestingly showed similar activities against negatively charged POPG LUVs (Fig. 1C). It raises the possibility that GsMTx-4 would exhibit the antimicrobial activity because the outermost leaflet of prokaryotic membranes is populated by phospholipids with negatively charged headgroups (see below).

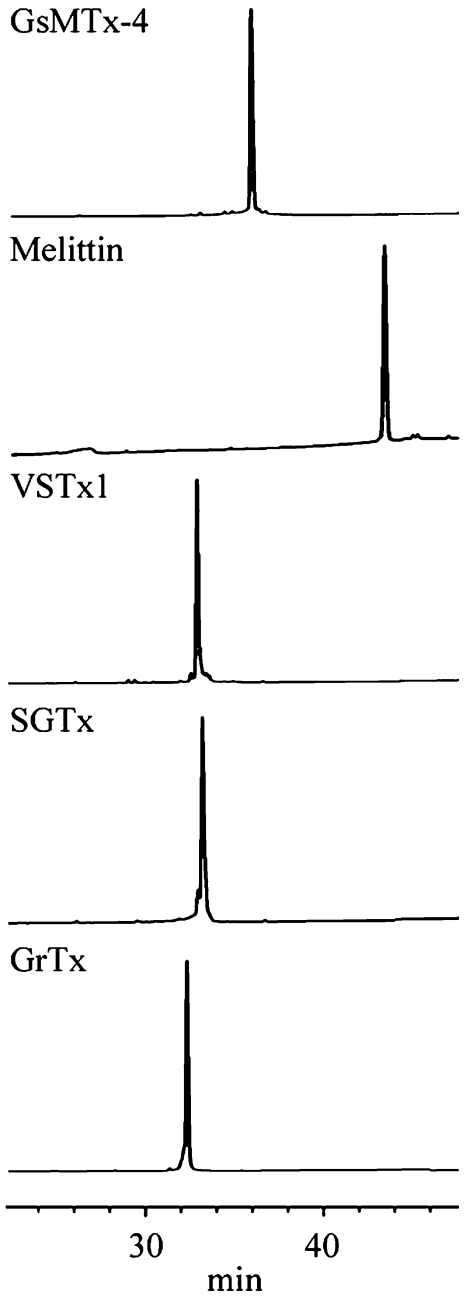

Fig. 3. RP-HPLC chromatograms of purified synthetic toxins. Toxins were eluted with a linear gradient from 20% to 60% mobile-phase B (100% acetonitrile; 0.1% TFA) over 40 min at a flow rate of 1 ml/min, where mobile-phase A was 0.1% TFA in water.

Antimicrobial activity of GsMTx-4

The antimicrobial effects of GsMTx-4 are summarized in Table 1. Interestingly we found that GsMTx-4 showed the antimicrobial activity and was especially more active against Gram-positive (*B. subtilis* 0.5 μM; *S. epidermidis* 4–8 μM; *Staphylococcus aureus* 2–4 μM) than Gram-negative bacteria (*P. aeruginosa* 8–16 μM; *S. typhimurium* 32–64 μM; and *E. coli* 8–16 μM). Although we need more investigation into the different activities of GsMTx-4 between Gram-positive and Gram-negative bacteria, there

Table 1
Antimicrobial activity of GsMTx-4

	Bacteria	MIC (μM)[a]	
		GsMTx-4 ($n = 6$)[b]	Melittin ($n = 3$)
Gram-positive	*Bacillus subtilis*	0.5	1
	Staphylococcus epidermidis	4–8	1–2
	Staphylococcus aureus	2–4	1–2
Gram-negative	*Psudomonas aeruginosa*	8–16	2
	Salmonella typhimurium	32–64	4
	Escherichia coli	8–16	2–4

[a] MIC : minimal inhibitory concentration.
[b] n = number of trials.

are two possibilities of the antimicrobial activity. One possibility is that GsMTx-4 likely acts by altering the membrane phospholipid packing in a manner similar to other antimicrobial peptides that act by disrupting the cell membrane. That GsMTx-4 is amphipathic like other antimicrobial peptides and more sensitive to negatively charged membranes than to zwitterionic ones (Figs. 1 and 2) is consistent with GsMTx-4's observed antimicrobial activity. The other possibility is that GsMTx-4 might act by modulating the gating of MS channels expressed by the tested bacterial cells. MS channels are widely distributed among both prokaryotes and eukaryotes with various functions [26–29]. Indeed, at all the bacteria tested so far, MS channels have been ascertained, except for only *S. epidermidis* [30]. However, because of no sequence information of the channels in higher organisms, we might hardly expect functional or structural differences of MS channels between eukaryotic and prokaryotic cells. Thus, the effect of GsMTx-4 against prokaryotic MS channel remains to be identified.

Structure–function relationship of toxins

Fig. 4 shows the primary and tertiary structures of GsMTx-4 and four other gating modifier toxins (VSTx1, HaTx, SGTx, and GrTx). HaTx and SGTx inhibit voltage-gated K^+ channels [17,31–36], while GrTx inhibits voltage-gated K^+ and Ca^{2+} channels [19]. All of these toxins show the same disulfide connectivity Cys (I–IV), Cys (II–V), and Cys (III–VI), which comprises a cysteine knot motif. In addition, all of them share a common structural feature: one face of the molecule is almost exclusively hydrophobic, while the other is charged. However, despite their amphipathicity and structural similarity to GsMTx-4, other toxins showed little ability to release calcein from POPC:POPG (1:1) LUVS, which mimic the bacterial membrane (SGTx 49% at 16 μM; GrTx 42% at 16 μM; VSTx1 13% at 16 μM) (Fig. 1D). Consistent with their weak ability to disrupt LUVs, the gating modifier toxins tested showed little or no antimicrobial activity at concentrations up to 32 μM (Table 2). One possible explanation for these observations is that GsMTx-4 has a net charge of +6 (the carboxyl terminus is amidated), whereas the net charges

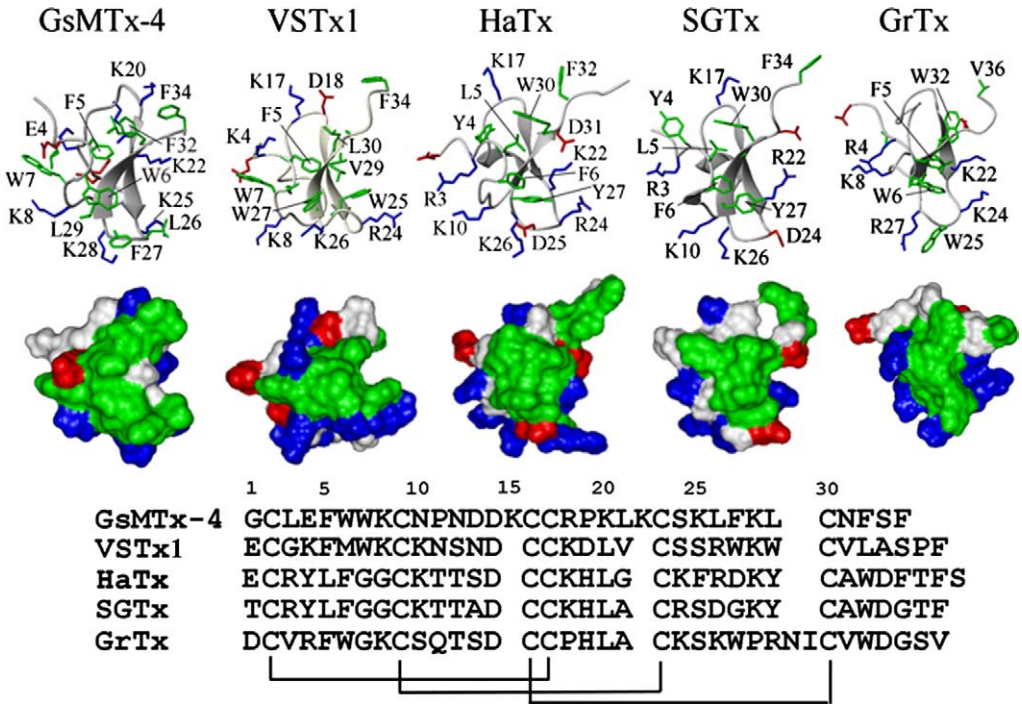

Fig. 4. Comparison of the distribution of the hydrophobic and charged residues on the surfaces of GsMTx-4, VSTx1, HaTx, SGTx, and GrTx. Hydrophobic, basic, and acidic residues are colored green, blue, and red, respectively. The structure topology of the antiparallel β-sheet was identified by MOLMOL. The coordinates of VSTx1, HaTx, SGTx, and GrTx were obtained from Protein Data bank entries 1S6X, 1D1H, 1LA4, and 1KOZ, respectively. Amino acid sequences of GsMTx-4, VSTx1, HaTx, SGTx, and GrTx are illustrated at the bottom. (For interpretation of the references to color in this figure legend, the reader is referred to the web version of this paper.)

Table 2
Antimicrobial activity of gating modifier toxins

Toxins	MIC (μM)	
	Bacillus subtilis	*Escherichia coli*
VSTx1	>32	>32
SGTx	>32	>32
GrTx	32	>32

of other gating modifiers are +2 (SGTx, HaTx, and GrTx) or +3 (VSTx1). In addition, the areas of the exposed hydrophobic regions are as follows; GsMTx-4, 747.8/3164.9 Å^2 (Phe5, Trp6, Trp7, Leu26, Phe27, Leu29, and Phe32); VSTx1, 576/3081.5 Å^2, (Phe5, Met6, Trp7, Val20, Trp25, Trp27, Val29, Leu30, and Ala31); HaTx, 596/3314.2 Å^2 (Tyr4, Leu5, Phe6, Tyr27, Ala29, and Trp30); SGTx, 581.7/3002 Å^2 (Tyr4, Leu5, Phe6, Ala20, Try27, Ala29, and Trp30); and GrTx, 606.1/3240.8 Å^2 (Phe5, Trp6, Ala20, Trp25, Pro26, Val31, and Trp32). Our findings suggest GsMTx-4 is organized such that it exerts a greater electrostatic and hydrophobic force than the other gating modifiers. Indeed, GsMTx-4 was retained longer than the other toxins on RP-HPLC (Fig. 3). K^+ channels are widespread and found in nearly all the free-living bacteria, archaea, and eukarya [37]. However, sequence of S3 and S4 helices within the voltage-sensing domain of the channels interacting with gating modifier toxins, such as VSTx1, HaTx, SGTx, and GrTx, is not well conserved between in prokaryotes and eukaryotes [37]. It would be one of the reasons for no antimicrobial activity of the gating modifiers except GsMTx-4.

Acknowledgments

This study was supported by grants from the Korea Science and Engineering Foundation through the Research Center for Proteineous Materials, the Molecular and Cellular BioDiscovery Research Program, the Brain Research Center of the 21st Century Frontier Research Program (M103KV010004 03K2201 00430), and the Development of Marine Novel Compounds program of the Korean Ministry of Maritime Affairs and Fisheries. H.J.J. and S.K.L. are supported in part by the Korean Ministry of Education (Brain Korea 21 program).

References

[1] T.M. Suchyna, J.H. Johnson, K. Hamer, J.F. Leykam, D.A. Gage, H.F. Clemo, C.M. Baumgarten, F. Sachs, Identification of a peptide toxin from *Grammostola spatulata* spider venom that blocks cation-selective stretch-activated channels, Gen. Physiol. 115 (2000) 583–598.
[2] F. Bode, F. Sachs, M.R. Franz, Tarantula peptide inhibits atrial fibrillation, Nature 409 (2001) 35–36.
[3] T. Osaki, M. Omotezako, R. Nagayama, M. Hirata, S. Iwanaga, J. Kasahara, J. Hattori, I. Ito, H. Sugiyama, S. Kawabata, Horseshoe crab hemocyte-derived antimicrobial polypeptides, tachystatins, with sequence similarity to spider neurotoxins, J. Biol. Chem. 274 (1999) 26172–26178.

[4] N. Fujitani, S. Kawabata, T. Osaki, Y. Kumaki, M. Demura, K. Nitta, K. Kawano, Structure of the antimicrobial peptide tachystatin A, J. Biol. Chem. 277 (2002) 23651–23657.
[5] R.J. French, S.C. Dudley Jr., Pore-blocking toxins as probes of voltage-dependent channels, Methods Enzymol. 294 (1999) 575–605.
[6] K.H. Ott, S. Becker, R.D. Gordon, H. Ruterjans, Solution structure of mu-conotoxin GIIIA analysed by 2D-NMR and distance geometry calculations, FEBS Lett. 278 (1991) 160–166.
[7] J.M. Hill, P.F. Alewood, D.J. Craik, Three-dimensional solution structure of mu-conotoxin GIIIB, a specific blocker of skeletal muscle sodium channels, Biochemistry 35 (1996) 8824–8835.
[8] F. Bontems, C. Roumestand, B. Gilquin, A. Menez, F. Toma, Refined structure of charybdotoxin: common motifs in scorpion toxins and insect defensins, Science 254 (1991) 1521–1523.
[9] J.H. Davis, E.K. Bradley, G.P. Miljanich, L. Nadasdi, J. Ramachandran, V.J. Basus, Solution structure of omega-conotoxin GVIA using 2-D NMR spectroscopy and relaxation matrix analysis, Biochemistry 32 (1993) 7396–7405.
[10] T. Kohno, J.I. Kim, K. Kobayashi, Y. Kodera, T. Maeda, K. Sato, Three-dimensional structure in solution of the calcium channel blocker omega-conotoxin MVIIA, Biochemistry 34 (1995) 10256–10265.
[11] S. Farr-Jones, G.P. Miljanich, L. Nadasdi, J. Ramachandran, V.J. Basus, Solution structure of omega-conotoxin MVIIC, a high affinity ligand of P-type calcium channels, using 1H NMR spectroscopy and complete relaxation matrix analysis, J. Mol. Biol. 248 (1995) 106–124.
[12] C.S. Anderson, R. Makinnon, C. Smith, C. Miller, Charybdotoxin block of single Ca^{2+}-activated K^+ channels. Effects of channel gating, voltage, and ion strength, J. Gen. Physiol. 91 (1988) 317–333.
[13] R. Mackinnon, C. Miller, Mechanism of charybdotoxin block of the high-conductance, Ca^{2+}-activated K^+ channel, J. Gen. Physiol. 91 (1988) 335–349.
[14] C.S. Park, C. Miller, Interaction of charybdotoxin with permeant ions inside the pore of a K^+ channel, Neuron 9 (1992) 307–313.
[15] H. Takahashi, J.I. Kim, H.J. Min, K. Sato, K.J. Swartz, I. Shimada, Solution structure of hanatoxin1, a gating modifier of voltage-dependent K(+) channels: common surface features of gating modifier toxins, J. Mol. Biol. 297 (2000) 771–780.
[16] K. Takeuchi, E. Park, C. Lee, J.I. Kim, H. Takahashi, K.J. Swartz, I. Shimada, Solution structure of omega-grammotoxin SIA, a gating modifier of P/Q and N-type Ca(2+) channel, J. Mol. Biol. 321 (2002) 517–526.
[17] C.W. Lee, S. Kim, S.H. Roh, H. Endoh, Y. Kodera, T. Maeda, T. Kohno, J.M. Wang, K.J. Swartz, J.I. Kim, Solution structure and functional characterization of SGTx1, a modifier of Kv2.1 channel gating, Biochemistry 43 (2004) 890–897.
[18] Y. Jiang, V. Ruta, J. Chen, A. Lee, R. MacKinnon, The principle of gating charge movement in a voltage-dependent K+ channel, Nature 423 (2003) 42–48.
[19] Y. Li-Smerin, K.J. Swartz, Gating modifier toxins reveal a conserved structural motif in voltage-gated Ca2+ and K+ channels, Proc. Natl. Acad. Sci. USA 95 (1998) 8585–8589.
[20] S.Y. Lee, R. MacKinnon, A membrane-access mechanism of ion channel inhibition by voltage sensor toxins from spider venom, Nature 430 (2004) 232–235.
[21] T.M. Suchyna, S.E. Tape, R.E. Koeppe 2nd, O.S. Andersen, F. Sachs, P.A. Gottlieb, Bilayer-dependent inhibition of mechanosensitive channels by neuroactive peptide enantiomers, Nature 430 (2004) 235–240.
[22] S.I. Sukharev, B. Martinac, V.Y. Arshavsky, C. Kung, Two types of mechanosensitive channels in the *Escherichia coli* cell envelope: solubilization and functional reconstitution, Biophys. J. 65 (1993) 177–183.
[23] C.C. Hase, A.C. Le Dain, B. Martinac, Purification and functional reconstitution of the recombinant large mechanosensitive ion channel (MscL) of *Escherichia coli*, J. Biol. Chem. 270 (1995) 18329–18334.
[24] B. Martinac, J. Adler, C. Kung, Mechanosensitive ion channels of *E. coli* activated by amphipaths, Nature 15 (1990) 261–263.
[25] E. Perozo, A. Kloda, D.M. Cortes, B. Martinac, Physical principles underlying the transduction of bilayer deformation forces during mechanosensitive channel gating, Nat. Struct. Biol. 9 (2002) 696–703.
[26] M. Kanzaki, M. Nagasawa, I. Kojima, C. Sato, K. Naruse, M. Sokabe, H. Iida, Molecular identification of a eukaryotic, stretch-activated nonselective cation channel, Science 285 (1999) 882–886.
[27] F. Maingret, M. Fosset, F. Lesage, M. Lazdunski, E. Honore, TRAAK is a mammalian neuronal mechano-gated K+ channel, J. Biol. Chem. 274 (1999) 1381–1387.
[28] N. Levina, S. Totemeyer, N.R. Stokes, P. Louis, M.A. Jones, I.R. Booth, Protection of *Escherichia coli* cells against extreme turgor by activation of MscS and MscL mechanosensitive channels: identification of genes required for MscS activity, EMBO J. 18 (1999) 1730–1737.
[29] A.F. Batiza, M.M. Kuo, K. Yoshimura, C. Kung, Gating the bacterial mechanosensitive channel MscL in vivo, Proc. Natl. Acad. Sci. USA 99 (2002) 5643–5648.
[30] S. Sukharev, S.R. Durell, H.R. Guy, Structural models of the MscL gating mechanism, Biophys. J. 81 (2001) 917–936.
[31] K.J. Swartz, R. Mackinnon, Hanatoxin modifies the gating of a voltage-dependent K+ channel through multiple binding sites, Neuron 18 (1997) 665–673.
[32] K.J. Swartz, R. Mackinnon, Mapping the receptor site for hanatoxin, a gating modifier of voltage-dependent K+ channels, Neuron 18 (1997) 675–682.
[33] Y. Li-Smerin, K.J. Swartz, Localization and molecular determinants of the Hanatoxin receptors on the voltage-sensing domains of a K(+) channel, J. Gen. Physiol. 115 (2000) 673–684.
[34] Y. Li-Smerin, K.J. Swartz, Helical structure of the COOH terminus of S3 and its contribution to the gating modifier toxin receptor in voltage-gated ion channels, J. Gen. Physiol. 117 (2001) 205–218.
[35] H.C. Lee, J.M. Wang, K.J. Swartz, Interaction between extracellular Hanatoxin and the resting conformation of the voltage-sensor paddle in Kv channels, Neuron 40 (2003) 527–536.
[36] J.M. Wang, S.H. Roh, S. Kim, C.W. Lee, J.I. Kim, K.J. Swartz, Molecular surface of tarantula toxins interacting with voltage sensors in K(v) channels, J. Gen. Physiol. 123 (2004) 455–467.
[37] M.M. Kuo, W.J. Haynes, S.H. Loukin, C. Kung, Y. Saimi, Prokaryotic K(+) channels: from crystal structures to diversity, FEMS Microbiol. 29 (2005) 961–985.